*Pure & Appl. Chem.*, Vol. 59, No. 10, pp. 1247–1252, 1987.
Printed in Great Britain.


# Magnetic ordering induced Raman scattering in $FePS_3$ and $NiPS_3$ layered compounds

M. Balkanski, M. Jouanne and M. Scagliotti

Laboratoire de Physique des Solides, Laboratoire Associé au C.N.R.S. L.A. 154, Université Pierre et Marie Curie, 4, Place Jussieu, 75252 PARIS CEDEX 05, France
and Centro Informazioni Studi Esperienze, P. O. Box 12081, 20134 MILANO, Italia

Abstract - Systematic investigation of the phonon Raman scattering efficiency in $FePS_3$ as a function of temperature in the vicinity of the magnetic phase transition temperature T demonstrates three levels of enhancement of the Raman peaks: i) in the low frequency region the appearance, and strong enhancement in the antiferromagnetic phase, of peaks not observable in the paramagnetic phase; ii) in the intermediate frequency region the enhancement and narrowing of peaks which are only weak in the paramagnetic phase; iii) in the high frequency region the enhancement of phonon Raman peaks. All of these manifestations can be explained by the Brillouin Zone folding due to the appearance, below $T_N$, of a magnetic superstructure in the c direction with a magnetic unit cell which is double that of the crystallographic cell. In $NiPS_3$ the antiferromagnetic in-plane ordering along the b axes conserves the same magnetic unit cell as the crystallographic cell. The magnetic ordering in the c and a directions is ferromagnetic. Only slight enhancements are observed in this case near $T_N$, but there also appear a broad continuum in the Raman spectrum and Fano interferences on top of this continuum.

## INTRODUCTION

The effect of magnetic ordering on the temperature variation of phonon Raman intensities has been first observed (ref. 1) in the ferromagnetic semiconducting spinels $CdCr_2S_4$ and $CdCr_2Se_4$. It has been found that certain lines of particular symmetries due to Raman active phonon modes exhibit an abrupt decrease of integrated intensity with increasing temperature through the Curie temperature Tc.

A theory of the spin-dependent phonon Raman scattering in magnetic crystals has been developed by Suzuki and Kamimura (ref. 2). A phenomenological treatment shows that the spin-dependent part of the integrated Raman intensity, expressed as a function of temperature, is proportional to the nearest neighbor spin correlation function. Two types of microscopic spin dependent scattering mechanisms, variation of the d electron transfer with lattice vibrations and the non-diagonal exchange interaction, are considered.

The effects of magnetic ordering on the phonon Raman scattering are different from those related to the direct excitation of the spin systems such as the light scattering by spin waves (ref. 3).

In materials where the microscopic mechanism for the spin-dependent Raman scattering can be attributed to the variation of the d electron transfer energy due to the relative displacement of the ions, the intermediate state interaction is considered under the assumption that the adsorption edge corresponds to a charge transfer transition from the d level to the conduction band. This suggests that the anomalous temperature dependence of intensity of the specific phonon lines would have a resonance enhancement when the energy of the excitation light corresponds to that of electronic transition, in addition to the magnetic ordering effect. Resonance effects on the spin dependent phonon Raman scattering have been observed (ref. 4) in $CdCr_2S_4$ and $CdCr_2Se_4$.

In addition to the resonance Raman scattering associated with the valence to conduction band transition a temperature dependent resonance enhancement occurs with the onset of ferromagnetic order, due to the spin splittings of the electronic band structure (ref. 5).

In another class of magnetic semiconductors, the europium chalcogenides, spin-dependent Raman scattering due to simultaneous excitation of the spin and phonon systems has been observed. The symmetry forbidden first order phonon Raman scattering, in the paramagnetic

phase of these NaCl structure-type materials, has been shown to be spin-disorder induced (ref. 6). In the ordered magnetic phases of EuSe and EuTe new peaks in the Raman spectra appear with intensities dependent on the temperature and applied magnetic field. The appearance of first order Raman scattering which is expected to be symmetry-forbidden is related to the folding of the Brillouin zone due to the magnetic superstructure (ref. 7).

Brillouin zone folding effects of the phonon branches in the antiferromagnetic phase of $VI_2$ are also observed (ref. 8) and attributed to the phonon modulation of the antiferromagnetic exchange interaction between the $V^{2+}$ spins.

We report here recent light scattering experiments performed on layered materials, $MPS_3$ with M = Ni and Fe.

When the Néel transition temperature is approached from above, entering from the paramagnetic into the antiferromagnetic phase in $FePS_3$ three effects are observed on the Raman line intensities in the low frequency part of the spectrum. The first is the appearance of Raman lines which are not observed in the paramagnetic phase. The second is a considerable enhancement of the integrated intensity and narrowing of certain lines which were weak and broad in the paramagnetic phase. The third is a relative enhancement and narrowing of lines present in the spectrum of the paramagnetic phase. In the antiferromagnetic phase of $FePS_3$ with successive layers having antiparallel spin ordering, the magnetic unit cell along the c axes is double that of the chemical cell. The observed enhancement of the Raman intensity is related to the Brillouin zone folding.

In $NiPS_3$ the effects of the magnetic ordering on the Raman spectrum are quite different. Crossing $T_N$ upon entering the magnetically ordered phase a broad band appears in the Raman spectrum, and the line shapes of the bands appearing on top of the broad band continuum show interference deformations. Some Raman lines are slightly enhanced and narrowed.

## STRUCTURE

The $FePS_3$ and $NiPS_3$ phases crystallize in the monoclinic symmetry, space group C2/m. The structure consists essentially of sulfur in a cubic close-packed array. Every other layer of octahedral sites is filled by the transition metal ions and the phosphorus atom pairs $P_2$. The structure (ref. 9) projection along the b axis is shown in Figure 1a. This structure clearly shows alternating slabs and Van der Waals gaps. The Van der Waals gap for the first transition metal row compounds remains fairly constant at 3.24 Å. It is much wider than in the $MS_2$ compounds. The monoclinic unit cell contains a single layer and four formula units.

The magnetic structure of $NiPS_3$ (ref. 10) and $FePS_3$ (ref. 11) were determined by neutron diffraction. For $NiPS_3$ this structure can be described, in a two dimentional layer, by the presence of double parallel ferromagnetic chains antiferromagnetically coupled to each other the moments being oriented in the $\vec{c}$ direction: type I in Figure 1b. For $FePS_3$ the chains of a plane are also antiferromagnetically coupled to those of the neighbouring planes, implying a doubling of the c parameter of the magnetic cell: type II in Figure 1c.

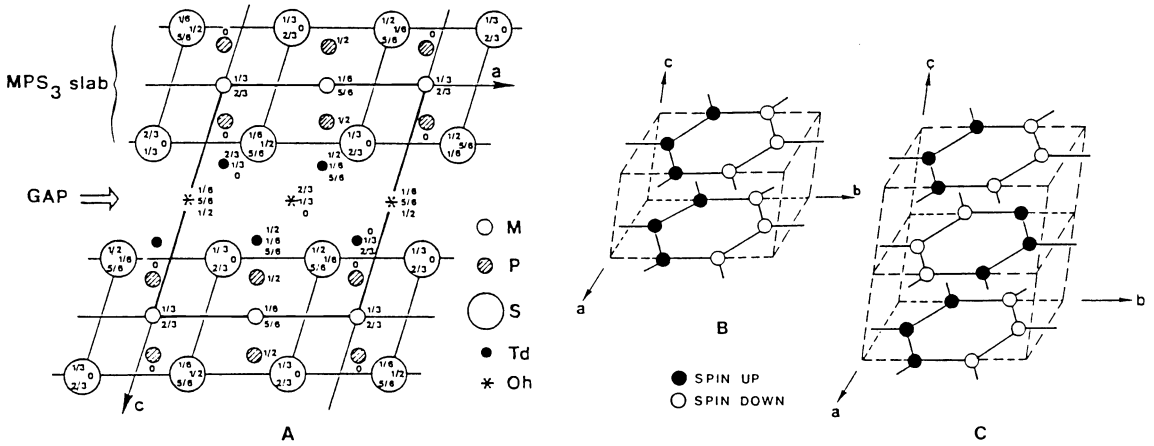


Fig. 1. Projection of the $MPS_3$ structure along the b axis (A) from ref. 9. Magnetic structures presented by the Ni (B) and by the Fe (C) in the $MPS_3$ layered compounds, from ref. 10.

## EXPERIMENTAL RESULTS

Light scattering experiments are carried out on cleaved single crystals of $NiPS_3$ and $FePS_3$ (ref. 12,13). The Raman spectra are excited by the 476.5 nm and 488.0 nm lines of an $Ar^+$ laser in a quasi backscattering geometry with the laser beam at Brewster incidence. The scattered light is dispersed by means of a double grating Coderg PH 1 spectrometer and the signal is analyzed by a conventional photon counting system. Typical Raman spectra of $FePS_3$ recorded at liquid helium temperature and at room temperature are shown in Figure 2. Some significant differences are observed upon comparing these two spectra. At low temperature two strong narrow peaks at 88 $cm^{-1}$ and 95 $cm^{-1}$ and a weaker one at 108 $cm^{-1}$ appear in the spectral region where only a weak broad band is detected at room temperature. A new peak appears also at 161 $cm^{-1}$ at low temperature. As the temperature is lowered the peaks at 249 $cm^{-1}$ and 380 $cm^{-1}$ are considerably enhanced. The temperature variation of the normalized intensity of the peaks at 88 $cm^{-1}$, 249 $cm^{-1}$ and 380 $cm^{-1}$ is represented in Figure 3. The Néel temperature of $FePS_3$ is 118 K. The intensity of the 88 $cm^{-1}$ peak rises abruptly below $T_N$ without any frequency variation, the intensity of the peak at 249 $cm^{-1}$ is significantly enhanced when passing through $T_N$ while the intensity of the peak at 380 $cm^{-1}$ changes only slightly. The band widths of all these three peaks undergo significant broadening when crossing the Néel temperature going from the antiferromagnetic to the paramagnetic phase. This variation is shown in Figure 4.

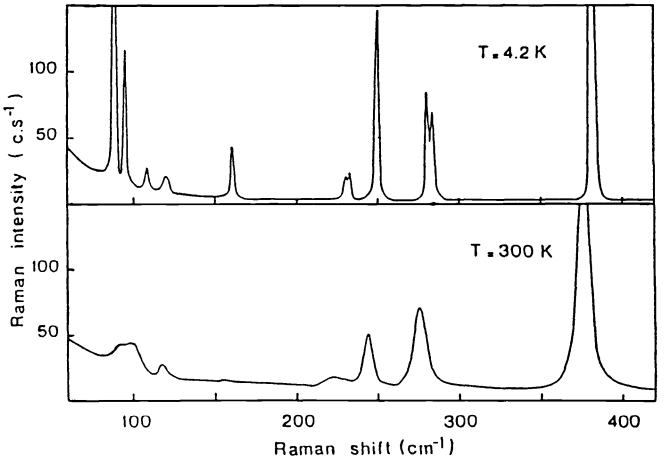


Fig. 2.
Raman spectra of iron phosphorus trisulfide excited with the 476.5 nm line of an $Ar^+$ laser and recorded at 300 K and at 4.2 K, from ref. 12.

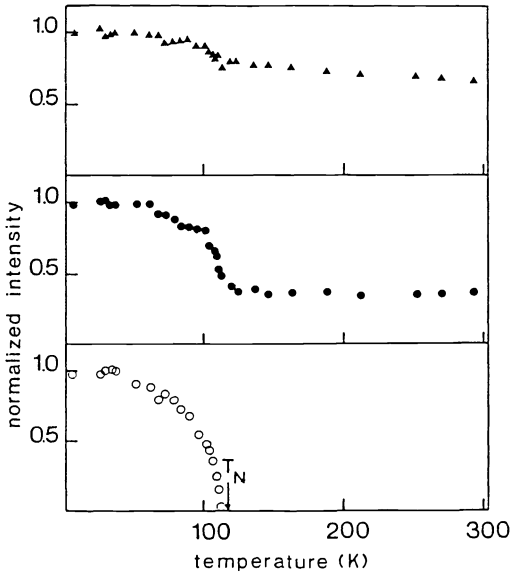


Fig. 3. Reduced integrated intensities of the peaks at 88 $cm^{-1}$ (○), 249 $cm^{-1}$ (●) and 380 $cm^{-1}$ (▲) recorded at different temperatures and corrected for the Bose population factor (ref. 13).

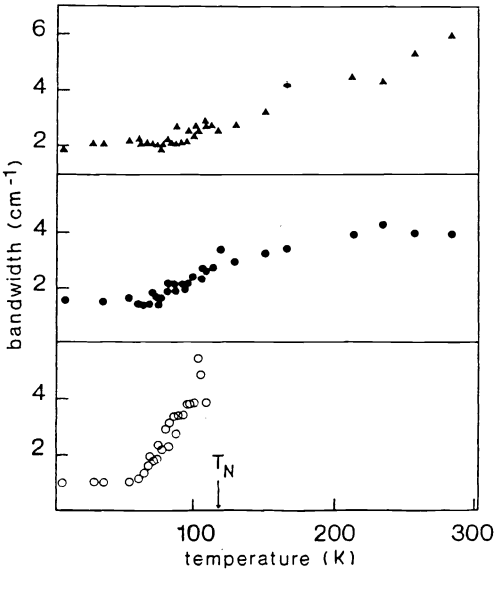


Fig. 4. Temperature dependence of the bandwidths of the peaks at 88 $cm^{-1}$ (○), 249 $cm^{-1}$ (●) and 380 $cm^{-1}$ (▲) in the Raman spectrum of $FePS_3$ (ref. 13).

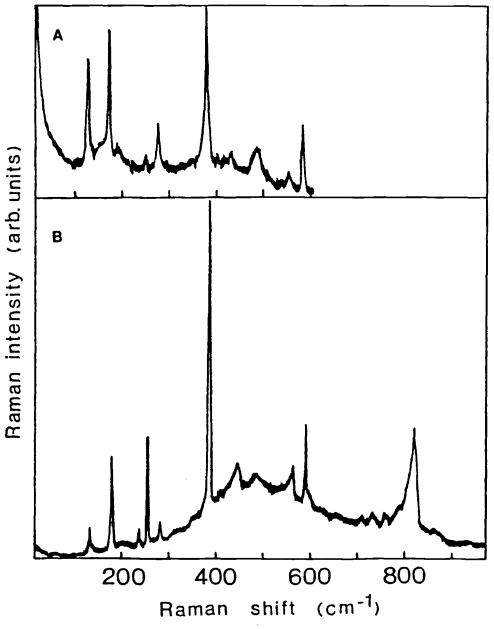


Fig. 5. Raman spectrum of nickel phosphorus trisulfide recorded at room temperature and at liquid nitrogen temperature with the 514.5 nm line of an $Ar^+$ laser as exciting source.

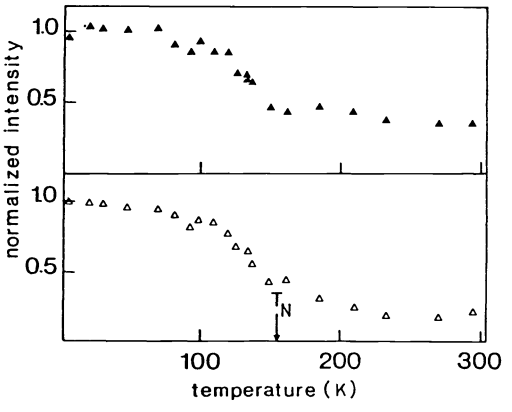


Fig. 6. Temperature dependence of the integrated intensity of the 387 $cm^{-1}$ peak of nickel phosphorus trisulfide (▲) and the broad band detected around 500 $cm^{-1}$ (Δ).

Raman spectra of $NiPS_3$ recorded at room temperature and liquid nitrogen temperature are shown in Figure 5. The Néel temperature of $NiPS_3$ is 155 K (ref. 14). The temperature dependence of the reduced intensity of the peak at 387 $cm^{-1}$ and the broad band at 500 $cm^{-1}$ is reported in Figure 6. The variation of the Raman intensity for $NiPS_3$ when crossing the Néel temperature is quite comparable to that observed for $FePS_3$.

## DISCUSSION

The peaks observed at low frequency depend on the cation substitution and therefore involve vibrational modes in which the motion of the $M^{2+}$ ion is important while the spectral pattern in the high frequency region is insensitive to the metal cation substitution and can be interpreted in terms of normal modes of the staggered $P_2S_6$($D_{3d}$ group) unit (ref. 12,13).

The most striking effect observed in these experiments is the strong enhancement of some Raman lines, mainly in the low frequency region. The observed enhancements are clearly related to the magnetic ordering. The lines at 88, 95 and 108 $cm^{-1}$ strongly decrease in intensity without frequency shifts around $T_N$ (118 K) and range into a broad weak band at about 100 $cm^{-1}$ at higher temperature. The intensity of the line at 161 $cm^{-1}$ becomes so small that it is impossible to measure at temperature larger than $T_N$, while the intensity of the line at 249 $cm^{-1}$, which is strongly polarized, decreases.

On the contrary the band at 378 $cm^{-1}$/at room temperature due to the symmetric stretching of the $PS_3$ tetrahedra, as well as the lines at 277 and 222 $cm^{-1}$, due to $PS_3$ deformation and bending modes, exhibit only small changes in intensity around $T_N$.

Considering the fact that no frequency shift and anomalous line broadening accompany the anomalous enhancement of some of the Raman lines in the vicinity of the Néel temperature we can rule out the possibility of interpreting this effect as light scattering by spin waves (ref. 3).

In the experiments presented here using different exciting wavelengths in the spectral range 1.92 eV-2.71 eV no resonance effect has been detected for the peaks which exhibit strong temperature dependence. This observation rules out the possibility of relating the intermediate electronic states of the Raman process to the spin dependent transition (ref. 4) nor is it related to a band splitting into spin polarized subbands due to the onset of magnetic order (ref. 5).

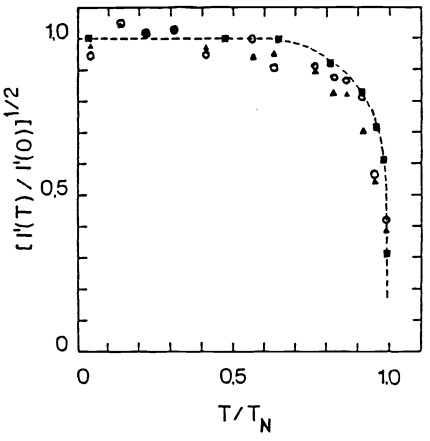


Fig. 7. The spin correlation function of $FePS_3$ evaluated from the temperature behavior of the line at 88 $cm^{-1}$ (O) and 161 $cm^{-1}$ (▲) using equation 1 (ref. 12). For comparison the square of the reduced magnetic moments taken from ref. 11 is reported (■). The broken line is shown as an eye guide.

The phenomenological theory developed by Suzuki and Kamimura (ref. 2) gives the spin-dependent phonon Raman scattering in magnetic crystals in terms of the correlation function of the spin dependent polarizability tensors. The temperature dependence of the reduced integrated intensity is thus given by

$$I(T) = |R + M \langle S_o . S_1 \rangle / S^2|^2 \qquad (1)$$

R is the spin independent term, $M \frac{\langle S_o . S_1 \rangle}{S^2}$ is the spin dependent term of the Raman tensor and $\frac{\langle S_o . S_1 \rangle}{S^2}$ is the reduced nearest neighbor spin correlation function.

The spin dependent Raman tensor has the same temperature dependence as the correlation function. This is true independently of the microscopic mechanism responsible for the scattering process.

The temperature dependence of the spin-dependent Raman intensity of the peaks at 88 and 161 $cm^{-1}$ is shown in Figure 7 (ref. 12) compared with the square of the reduced magnetic moment (ref. 11). Both functions are constant up to 0.6 - 0.7 $T_N$ and then abruptly decrease approaching the transition temperature, in agreement with the 2D Ising character of $FePS_3$ (ref. 11).

The magnetic ordering induced Raman scattering is to a large extent related to the Brillouin zone folding due to the fact that the magnetic unit cell in the c direction is double that of the chemical cell. The folding of the phonon dispersion curves due to the magnetic superstructure brings zone bondary phonons to the center of the Brillouin zone rendering this phonon Raman active. The appearance of the two strong and narrow bands at 88 $cm^{-1}$ and 95 $cm^{-1}$ can be seen to originate from folded acoustic branches by comparison with the phonon dispersion curves of a similar compound, iron dichloride (ref. 15). The enhancement of the intensity of the peak at 161 $cm^{-1}$ may come from the folding of the infrared active branch at 153 $cm^{-1}$ (ref. 16).

The Raman spectra of $NiPS_3$ given in Figure 5 show somewhat different behavior from that of $FePS_3$. The magnetic structure of this compound does not lead to any change of the c parameter of the magnetic cell. The magnetic cell coincides with the crystalline one. The Raman enhancement due to the spin ordering in $NiPS_3$ is different in nature from that observed for $FePS_3$. It is related to the spin correlation of the in plane chains. No spectacular effect is observed in the low frequency region, but enhancements of the peaks assigned to $P_2S_6$ normal modes occur. Moreover, an anomalously broad band extending from 300 $cm^{-1}$ to 900 $cm^{-1}$ appears. The peaks at 448 $cm^{-1}$ and 565 $cm^{-1}$ exhibit a Fano type interference with this broad band.

## CONCLUSION

Comparison of the light scattering data obtained on two systems, $FePS_3$ and $NiPS_3$, having the same crystallographic structure but different magnetic ordering reveals different behavior in the spin-ordering induced Raman scattering.

For $FePS_3$ the lack of significant frequency shift and anomalous line broadening of the low frequency, most strongly enhanced Raman peaks in the vicinity of the magnetic ordering transition temperature rules out direct spin wave excitations. The non-observation of resonance behavior, for excitation energies close to the electronic transitions of the peaks enhanced by the magnetic ordering indicates that the intermediate state is not a spin dependent function.

The most striking enhancement of Raman peaks occurs for $FePS_3$ for which the magnetic superstructure doubles the crystallographic unit cell. This suggests that the Brillouin zone folding due to the magnetic superlattice along the c axis might be the reason for the observed three types of extraordinary enhancement of the phonon Raman intensity: i) the appearance of Raman peaks not observed in the paramagnetic phase, ii) the folding of the phonon branches back to the center of the Brillouin zone produces additional phonon density in the vicinity of modes which are only infrared active. The folded branch from the Brillouin zone edge has different symmetry properties, thus inducing some partial Raman activity. iii) Folding back flat Raman active branches increases the density of active modes in the center of the Brillouin zone and thus enhances the Raman intensity.

Neither of these three effects can be invoked for the enhancement of the Raman modes in $NiPS_3$ for which the magnetic superstructure coincides with the crystallographic unit cell. The magnetic ordering results in antiferromagnetic interaction among chains in the plane and ferromagnetic interplane interaction in the c direction. Here the effect on the Raman spectrum is the appearance of a very broad band which acts as a continuum in the interference with single modes producing a Fano type line shape deformation. Some normal modes are also enhanced. This enhancement may come through the microscopic mechanism involving the variation of the d electron transfer with lattice vibrations or that of non-diagonal exchange. The broad continuum of Raman scattering may be due to electronic transitions from split-off spin polarized subbands. It is possible that in this case the magnetic order influences only indirectly the phonon Raman scattering intensity via resonance effects due to spin splittings of the electronic band structure.

Further investigations are needed to elucidate the microscopic nature of the appearance of additional Raman activity in the magnetically ordered 2D systems.

## Acknowledgements

We are pleased to acknowledge stimulating discussions with Professor G. Benedek and Professor R. F. Wallis.

## REFERENCES

1. E. F. Steigmeier and G. Harbeke, Phys. Kondens. Materie, 12, 1 (1970).
2. N. Suzuki and H. Kamimura, J. Phys. Soc. Jpn., 35, 985 (1973).
3. P. A. Fleury, S. P. S. Porto, L. E. Cheesman and H. J. Guggenheim, Phys. Rev. Letters, 17, 84 (1966).
4. N. Koshizuka, Y. Yokoyama and T. Tsushima, Physica, 89B, 214 (1977).
5. N. Koshizuka, S. Ushioda, T. Tsushima, Phys. Rev., B21, 1316 (1980).
6. J. C. Tsang, M. S. Dresselhaus, R. L. Aggrawal, T. B. Reed, Phys. Rev., 9B, 984 (1974).
7. R. P. Silberstein, L. E. Schmutz, V. J. Tekippe, M. S. Dresselhaus, R. L. Aggarwal, Solid State Commun., 18, 1173 (1976).
8. G. Guntherodt, W. Bauhofer, G. Benedek, Phys. Rev. Lett., 43, 1427 (1979).
9. G. Ouvrard, R. Brec and J. Rouxel, Mat. Res. Bull., 20, 1181 (1985).
10. R. Brec, Solid State Ionics (to be published).
11. K. Kurosawa, S. Saito, Y. Yamaguchi, J. Phys. Soc. Jpn., 52, 3919 (1983).
12. M. Scagliotti, M. Jouanne, M. Balkanski and G. Ouvrard, Solid State Commun., 54, 291 (1985).
13. M. Scagliotti, M. Jouanne, M. Balkanski, G. Ouvrard, G. Benedek, Phys. Rev. B (submitted).
14. Y. Chabre, P. Segransan, C. Berthier, G. Ouvrard, in "Fast Ion Transport in Solids", P. Vashishta, J. N. Mundy, and G. K. Shenoy, Eds.), North-Holland, 1979, p. 221.
15. G. Benedek and A. Frey, Phys. Rev., B21, 266 (1980).
16. C. Sourisseau, J. P. Forgerit and Y. Mathey, J. Solid State Chem., 49, 134 (1983).